Stereoselectivity and Chemoselectivity in Ziegler−Natta Polymerizations of Conjugated Dienes. 1. Monomers with Low-Energy s-*Cis* η^4 Coordination§

Chiara Costabile,† Giuseppe Milano,† Luigi Cavallo,‡ and Gaetano Guerra*,†

Dipartimento di Chimica, Universita' di Salerno. Via Salvador Allende, I-84081 Baronissi, Salerno, Italy, Dipartimento di Chimica, Universita' "Federico II" di Napoli, and Complesso Monte S. Angelo I-80126, Napoli, Italy

Received April 17, 2001; Revised Manuscript Received July 23, 2001

ABSTRACT: The mechanisms of stereoselectivity and chemoselectivity in the Ziegler−Natta polymerizations of conjugated dienes have been investigated by density functional methods, in the framework of the widely accepted polymerization scheme involving *anti*-allyl coordination of the growing chain. Most insertions would occur through intermediates with the diene monomer s-*cis* η^4 coordinated to the metal and with the monomer concavity oriented toward the terminal allyl group of the growing chain. Monomer coordinated intermediates presenting a backbiting of the *anti*-allyl coordinated growing chain ($\eta^3\eta^2$) would essentially lead to 1,4-*unlike* insertions only, while monomer coordinated intermediates simply presenting an *anti*-allyl coordination of the growing chain would lead to 1,4-*like* and/or 1,2-*unlike* insertions. These models are able to rationalize several experimental data relative to stereoselectivity and chemoselectivity in Ziegler−Natta polymerizations of conjugated dienes.

Introduction

The polymerization of conjugated dienes with transition-metal catalytic systems is an insertion polymerization as is that of monoalkenes with the same systems. Moreover, it is nearly generally accepted that for diene polymerization the monomer insertion reaction occurs in the same two steps established for olefin polymerization by transition-metal catalytic systems: (i) coordination of the monomer to the metal, (ii) monomer insertion into a metal−carbon bond. However, the polymerization of dienes presents several peculiar aspects mainly related to the nature of the bond between the transition metal of the catalytic system and the growing chain, which is of σ type for the monoalkene polymerizations, while it is of the allylic type in the conjugated diene polymerizations.[1−10]

Several experimental facts have been rationalized in terms of different π-allyl insertion mechanisms, depending on the nature of the catalytic systems and of the diene monomer, mainly by the extensive work of Porri and co-workers, as reviewed in refs 8 and 9, and Taube and co-workers, as reviewed in ref 10. A widely accepted scheme for *cis*-1,4 and 1,2 polymerizations of conjugated dienes is reported in Scheme 1.[8−10] In particular, it has been suggested that 1,2 units and *cis*-1,4 units can derive from an intermediate including a s-*cis*-η^4 coordinated diene monomer as well as a η^3 coordinated allyl terminal of the growing chain presenting an *anti* structure.[7−9] This kind of arrangement of the ligands would give rise to *cis*-1,4 or to 1,2 units, depending on whether the incoming monomer reacts at the terminal C4′ or internal C2′ allyl carbon, respectively. The labels for the carbon atoms presented in Scheme 1 and used in the rest of the paper should help to visualize 1,4 and 1,2 enchainments.

Scheme 1

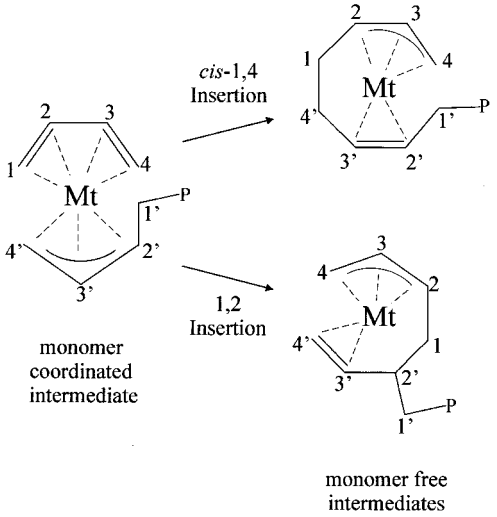

While in olefins polymerization the monomer free intermediates could be only stabilized by weak hydrogen agostic interactions (γ or β),[11] in dienes polymerization the monomer free intermediates could be stabilized by the higher coordination energies connected with the backbiting of double bonds present along the growing chain[10−14] (as sketched for the monomer free intermediates of Scheme 1). The existence of complexes with polydienyl chains coordinated to a transition metal through the terminal allyl group as well as by one or two double bonds along the chain (backbiting coordination) has been proved by NMR and X-ray diffraction studies.[15−19] Moreover, it is well-known that, also in the absence of cocatalysts, complexes containing backbiting π-allyl ligands can be active in the polymerization of conjugated dienes.[8,16,19]

According to the polymerization scheme proposed by Porri and co-workers,[8] the iso and syndiotactic isomerism in the insertion polymerization of dienes (for 1,2 polymerization of generic dienes and for *cis*-1,4 polym-

† Universita' di Salerno.
‡ Universita' "Federico II" di Napoli.
§ Dedicated to Prof. Umberto Giannini in recognition of his fundamental contribution in polymerization catalysis.

10.1021/ma010673h CCC: $20.00
Published on Web 10/13/2001

erization of 4 monosubstituted or of 1,4 disubstituted monomers) would be determined by the relative orientations of the two ligands (diene monomer and allyl terminal of the growing chain) in the preinsertion catalytic intermediates. Instead, according to a molecular mechanics study relative to the $CpTiCl_3$−MAO system reported by some of us, this isomerism could be related to the energy differences between monomer free intermediates.[13] Moreover, according to a recent density functional study, the rate-determining step would be the monomer coordination, associated with the removal of the backbiting of the growing chain,[14] rather than monomer insertion. This clearly indicates that both monomer coordination and monomer insertion reactions should be considered to rationalize the chemoselectivity and stereoselectivity in conjugated dienes polymerization.

Contrary to the case of monoalkene polymerization,[20,21] only few theoretical studies have been devoted to conjugated dienes polymerization.[12−14,22−25] Nevertheless, density functional studies have been focused on 1,4-butadiene polymerization with Ni(II)-based catalytic systems and, in particular, on the *cis*/*trans* stereoselectivity associated with the *anti*−*syn* isomerization of the allyl group of the growing chain.[23−25] Ab initio studies on butadiene and isoprene homopolymerization and copolymerization rates (and on the role of backbiting in determining reactivity) have been also reported.[22] As regards the chemoselectivity and iso/syndio stereoselectivity, only the already cited molecular mechanics study has been reported.[13] Hence, a detailed theoretical study of the mechanisms of chemoselectivity and stereoselectivity in the polymerization of conjugated dienes is still lacking. In this paper monomer free and monomer coordinated intermediates as well as transition states for monomer insertions have been investigated by density functional techniques. In particular, models that include or do not include an ancillary ligand besides the monomer and the growing chain are discussed. The corresponding monomer free species involve one or two backbiting double bonds, respectively.

It is worth noting that the s-*cis* η^4coordination of the diene monomer is energetically feasible (it has been observed in several metal complexes[26]) for the case of several dienes like butadiene, isoprene, (*E*)-pentadiene, and 2,3-methylbutadiene. This kind of coordination is instead of much higher energy and has not been observed for stable metal complexes of (*Z*)-pentadiene and 4-methylpentadiene, due to nonbonded interactions between the terminal methylenic group and a terminal methyl group. Moreover, for the latter monomers this kind of nonbonded repulsive interactions would be present also in the resulting *anti* allyl group. As a consequence, the models and the mechanism considered in this paper refer only to dienes with low-energy s-*cis* η^4 coordination. A paper describing a different polymerization mechanism for conjugated dienes presenting high-energy s-*cis* η^4 coordination is in preparation.

Models and Computational Details

Models. The assumed polymerization mechanism involves two intermediates and two transition states for each insertion reaction path. A first kind of intermediate corresponds to a monomer free species where the growing chain presents the reactive end *anti* η^3 coordinated, as well as one (see Scheme 1) or two double bonds η^2 coordinated. The second kind of intermediate is a monomer coordinated species presenting a s-*cis* η^4 coordinated diene and an *anti* η^3 coordination of the growing chain (see Scheme 1). It can be helpful to define the orientations of the *anti* η^3 coordinated allyl group and of the *cis* η^4 coordinated diene with respect to a third ligand L (which can be an ancillary ligand like cyclopentadienyl or a backbiting double bond) by the rotation angles around the axes connecting their center to the metal. In particular, as shown in Scheme 2, we assume $\phi = 0°$ when the concavity of the group is oriented in the opposite direction with respect to the L ligand (*endo* orientation) and $\phi = 180°$ when the concavity of the group is oriented in the L ligand direction (*exo* orientation).[13]

Scheme 2

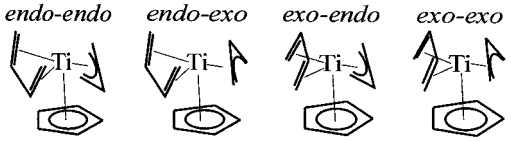

The assumption of monomer free and of monomer coordinated intermediates is widely accepted in the literature and is based on NMR and X-ray diffraction characterizations of π-allyl complexes, which show catalytic activity also in the absence of cocatalysts.[15−17,19,26,28−31] Moreover, possible isomerization of the *anti* allyl terminal of the growing chain toward the more stable *syn* allyl terminal, which in the framework of the π-allyl polymerization scheme could lead to the formation of 1,4 *trans* units,[10,23−25] has not been considered.

As in our previous paper,[13] the chirality of coordination of allyl groups and of double bonds is defined according to ref 27. As regards the chirality of double bond coordination in intermediates corresponding to 1,4 insertion, it is defined with reference to the carbon atom which is more distant along the chain with respect to the allyl group.

Because of the dependence of the results on the direction of monomer approach as well as to the difficulties to simulate the environment of the metal complex, transition states relative to the monomer coordination[14] have not been considered in the present paper.

Computational Details. Stationary points on the potential energy surface were calculated with the Amsterdam Density Functional (ADF) program system developed by Baerends et al.[32,33] The electronic configurations of the molecular systems were described by a triple-ζ STO basis set on Ni and Ti for 3s, 3p, 3d, 4s, and 4p. Double-ζ STO basis sets were used for C(2s,2p) and H(1s). The basis sets on C is augmented with a single 3d polarization function except for H, where a 2p function was used. The $1s^2 2s^2 2p^6$ configuration on nickel and titanium and $1s^2$ configuration on carbon were assigned to the core and treated within the frozen core approximation. Energetics and geometries were evaluated by using the local exchange-correlation potential by Vosko et al.[34] augmented in a self-consistent manner with Becke's[35] exchange gradient correction and Perdew's[36] correlation gradient correction. First-order scalar relativistic corrections were added to the total energy, since a perturbative relativistic approach is sufficient for 3d metals. In view of the fact that all Ni-based systems investigated in this work show a large HOMO−LUMO gap, a spin-restricted formalism was used for calculations on this kind of systems. As regards Ti systems, due to the open-shell character of the

systems under study an unrestricted formalism has been used.

All the structures that will follow are stationary points on the potential energy surface. Geometry optimizations were terminated if the largest component of the Cartesian gradient was smaller than 0.002 au. Transition-state geometries were approached by a linear-transit procedure, using the distance between the C(diene) and C(allyl) atoms which are going to form the new C−C bond as reaction coordinate, while optimizing all other degrees of freedom. Full transition-state searches were started from geometries corresponding to maxima along the linear-transit curves.

A considerable amount of related computational studies have contributed to the comprehension of fine details of olefins polymerizations with both early and late transition metals,[37] of styrene polymerization with Cp-based titanium catalysts,[38] and of butadiene polymerization with Ni(II)-based catalysts.[12,23−25]

A comparative computational study has shown that the DFT functional we have chosen is in excellent agreement with one of the best wave function-based methods available today to investigate polymerization reactions with Ziegler−Natta catalysts.[39] Further support to the reliability of the computational methodology comes out by the results of test calculations on the neutral complexes $Cp_2Ti(C_5H_9)$[40] and $CpZr(C_3H_5)(C_4H_6)$.[26] The most stable structures we calculated are very similar to those characterized by X-ray diffraction with maximum difference for the Mt−C distances of 0.1 Å. Experimental and calculated orthogonal coordinates can be found in the Supporting Information. As for the zirconium complex, the calculated energies of the diene−allyl *exo*−*exo*, *endo*−*endo*, *endo*−*exo*, and *exo*−*endo* geometries are 0.0, 0.5, 4.2, and 4.3 kcal/mol, respectively. The only slightly larger energy of the *endo*−*endo* complex is in good agreement with its formation by photolysis at −40 °C, as pointed out by NMR measurements.[26]

Results

Models Including an Ancillary Ligand (Mechanisms Involving One Backbiting Double Bond). *Monomer Free Species.* A full analysis of the conformations of diastereomeric monomer free intermediates has shown that the conformational requirements for the backbiting of an *anti* π-allyl chain are very strict.[13,18]

As for titanium complexes presenting as ancillary ligand a Cp group, the minimum-energy geometries of the diastereoisomeric monomer free intermediates are shown in Figure 1. The chiralities of coordination of the allyl groups (assumed to be *si*) and of the double bonds (*si* or *re*) are also indicated in Figure 1 to easily visualize the possible stereoregularity (iso or syndio) of the model chains. In fact, *like* and *unlike* chiralities would possibly lead to isotactic and syndiotactic enchainments, respectively. In particular, isotactic and syndiotactic stereoregularity could occur for all diene monomers in the case of 1,2 polymerization, while it would occur only for 4-alkyl-substituted and 1,4-alkyl-disubstituted dienes in the case of 1,4 polymerization. Incidentally, the models of the monomer free intermediates of Figure 1 present geometries as well as energy differences similar to those obtained by simple molecular mechanics calculations and shown in Figure 4C (1,4-*like*), 5C (1,2-*unlike*), 4B (1,4-*unlike*), and 5B (1,2-*like*) of ref 13.

Lower and similar energies correspond to the 1,4-*like* (**1a**) and 1,2-*unlike* (**1b**) intermediates. The higher

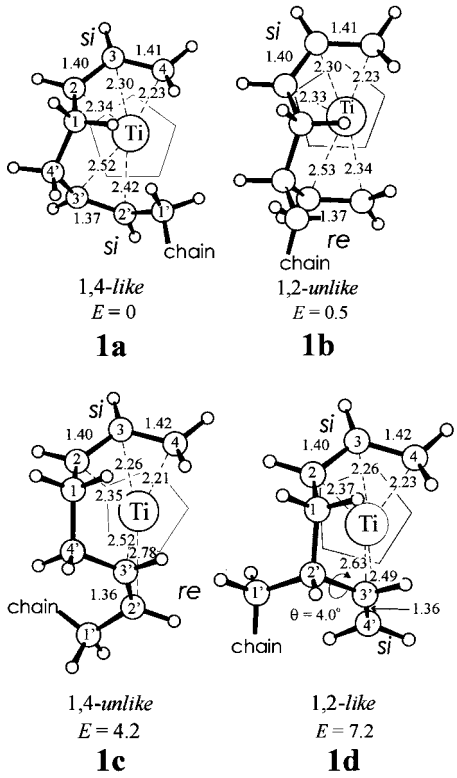

Figure 1. Minimum-energy geometries of the monomer free intermediates comprising an ancillary Cp ligand. The allylic-type chain end is η^3 coordinated to the metal, while the closest double bond of the chain is η^2 coordinated (backbiting) to the metal. Distances are in Å and energies are in kcal/mol.

energy of the 1,4-*unlike* (**1c**) and 1,2-*like* (**1d**) intermediates is associated with the orientation of the η^2 backbiting double bond, which is roughly orthogonal with respect to the allyl plane. In fact, similar calculations on a simplified model presenting coordination of an ethylene molecule, a Cp ring, and an allyl group have shown that an ethylene orientation nearly parallel to the allyl plane (similar to that one shown by the 1,4-*like* and 1,2-*unlike* intermediates **1a** and **1b**) is favored of about 5 kcal/mol with respect to geometries in which the ethylene was fixed nearly orthogonal with respect to the allyl plane (similar to that one shown by 1,4-*unlike* and 1,2-*like* intermediates **1c** and **1d**). The origin of this conformational preference is mainly electronic in nature, since no short distances between the different ligands were found in the high-energy geometries. Finally, the 1,2-*like* monomer free intermediate **1d** presents the highest energy due to the essentially eclipsed conformation around the central single bond of the C1′−C2′−C3′−C4′ dihedral, which leads to a short C1′−C4′ distance (2.99 Å).

With regard to the backbiting η^2 coordination of the double bond, it is generally symmetric. However, for the case of 1,4-*unlike* monomer free species **1c**, the C2′ atom is at a larger distance from the metal (C3′−Ti = 2.54 Å, C2′−Ti = 2.70 Å), due to steric interactions between the Cp and C1′ (with its substituents).

For the sake of comparison with the monomer coordinated intermediates of the next section, it is worth noting that, as a consequence of the backbiting, *endo* is the geometry of coordination of the allyl group in all the monomer free intermediates. That is, the concavity of the allyl group is oriented in the opposite direction with respect to the Cp ligand.

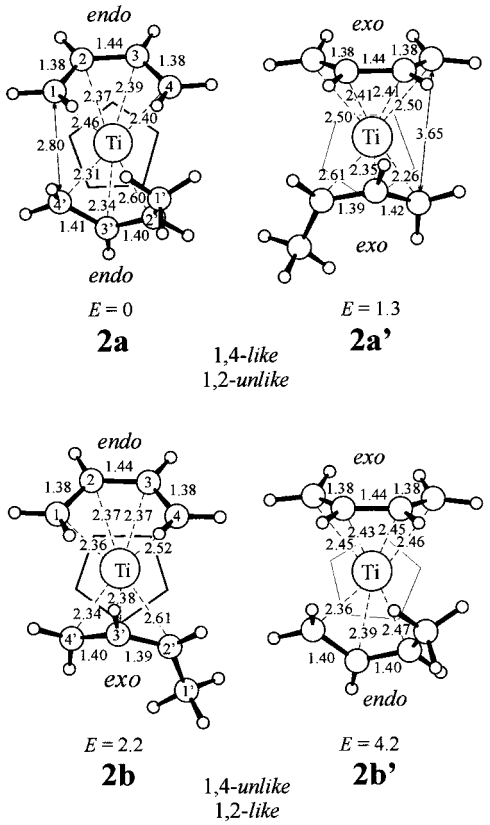

Figure 2. Minimum-energy geometries of the monomer coordinated intermediates comprising an ancillary Cp ligand. The allylic-type chain end is η^3 coordinated to the metal, while the butadiene is s-*cis* η^4-coordinated to the metal. Distances are in Å and energies are in kcal/mol.

Monomer Coordinated Species. In agreement with previous molecular mechanics calculations,[13] the minimum-energy geometries of the monomer coordinated intermediates present ϕ_{diene} and ϕ_{allyl} nearly equal to 0° or 180°. Hence, four possible minimum-energy intermediates are obtained, whose optimized geometry and energies are shown in Figure 2: $\phi_{diene} \approx \phi_{allyl} \approx 0°$ (*endo*−*endo*), $\phi_{diene} \approx 0°$ and $\phi_{allyl} \approx 180°$ (*endo*−*exo*), $\phi_{diene} \approx 180°$ and $\phi_{allyl} \approx 0°$ (*exo*−*endo*), $\phi_{diene} \approx \phi_{allyl} \approx 180°$ (*exo*−*exo*). Test calculations in which we fixed $\phi_{diene} \approx 90°$ resulted in optimized geometries that are roughly 13 kcal/mol higher in energy with respect to the most stable *endo*−*endo* monomer coordinated intermediate. The allyl of the growing chain results not symmetrically coordinated to the metal. In particular, for the four intermediates the terminal reactive allyl carbon is closer to the metal than the internal reactive one (2.26 < Ti−C4′ < 2.36 vs 2.45 < Ti−C2′ < 2.68 Å).

According to the polymerization scheme proposed by Porri and co-workers,[8] and as also indicated in Figure 2, diene insertion starting from the *endo*−*endo* **2a** and *exo*−*exo* **2a′** intermediates lead to 1,4-*like* or 1,2-*unlike* enchainments through C−C bond formation between the C1 of butadiene labeled as 1 in Figure 2 and C4′ of the allyl, and between the C1 of butadiene labeled as 4 and C2′ of the allyl, respectively. On the other hand, diene insertions starting from the *endo*−*exo* **2b** or *exo*−*endo* **2b′** intermediates lead to 1,4-*unlike* or 1,2-*like* enchainments, through C−C bond formation between the C1 of butadiene labeled as 1 and 4 and allyl atoms C4′ and C2′, respectively. Although the calculated energy differences are lower than those calculated for the monomer free species, also for the monomer coordinated species the intermediates which lead to 1,4-*like* and 1,2-*unlike* enchainments (i.e., *endo*−*endo* and *exo*−*exo*) are energetically favored with respect to intermediates which lead to 1,4-*unlike* and 1,2-*like* enchainments (i.e., *endo*−*exo* and *exo*−*endo*).

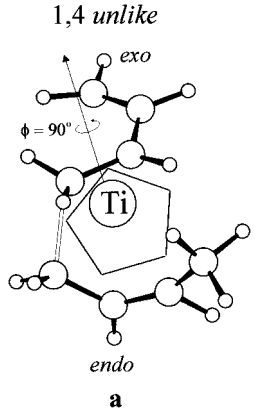

Figure 3. Example of a high-energy transition state obtained starting from intermediates with *exo* coordination of the monomer (**2a′** or **2b′**). The shown transition state would lead to the 1,4-*unlike* enchainment, starting from *exo*−*endo* monomer coordinated intermediate **2b′**.

The achievement of the minimum-energy monomer coordinated intermediate **2a** from the minimum-energy monomer free intermediates **1a** or **1b** implies a reduction of the energy of nearly 5 kcal/mol, due to the s-*cis* η^4 diene coordination which largely compensates the removal of the η^2 backbiting. Of course, an increase of free energy is expected as a consequence of the reduction of entropy associated with monomer coordination (see Discussion section). Moreover, the monomer coordinated species **2a** with *n*-inserted units is nearly 12 kcal/mol higher in energy with respect to the monomer free species **1a** or **1b** with $n + 1$ inserted units. Correspondingly, the energy differences between monomer free intermediates with *n* and $n + 1$ monomer units, that is, the energy reduction corresponding to both 1,4 and 1,2 insertions of butadiene into a polydienylic chain, are nearly 17 kcal/mol, in good agreement with the experimental values of the heats of polymerization ($\Delta H_{1,4cis}$ = 18.6 kcal/mol, $\Delta H_{1,2}$ = 17.4 kcal/mol).[41]

Transition States for Monomer Insertion. Each of the four monomer coordinated species of Figure 2 could give both 1,2 and 1,4 insertion. As a consequence, eight possible transition states have been considered. As regards the transition states corresponding to insertion of *exo* coordinated dienes (that is, the four transition states corresponding to the monomer coordinated intermediates **2a′** and **2b′**), they have been calculated to be more than 20 kcal/mol higher in energy with respect to the most stable *endo*−*endo* monomer coordinated species. In fact, in the case of insertion of *exo* coordinated dienes large distortions from the preinsertion geometry are required. For instance, the transition state for insertion of the *exo* coordinated monomer into the *endo* coordinated allyl requires a diene rotation from $\phi_{diene} \approx 0°$ to $\phi_{diene} \approx 90°$ (see Figure 3). It is worthy to note that situations with $\phi_{diene} \approx 90°$ were calculated to be of high energy also in the case of the monomer coordinated intermediates.

As regards the four transition states obtained from the intermediates presenting endo diene coordination, **2a** and **2b**, their geometries and relative energies are shown in Figure 4. Of course, 1,4 insertion has been

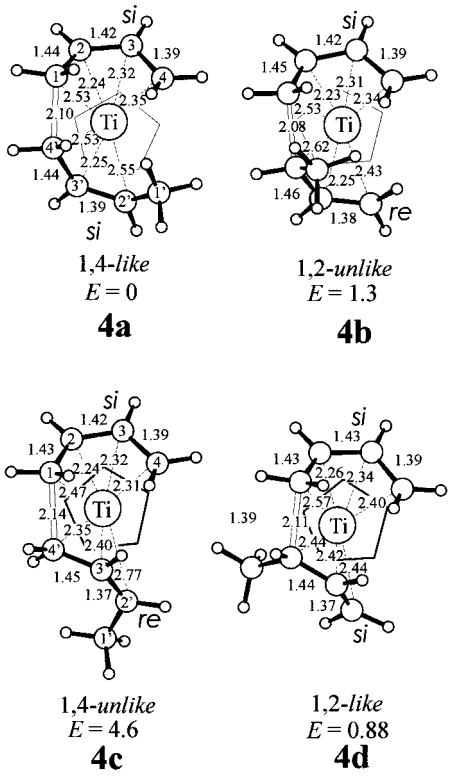

Figure 4. Geometries of the transition states that lead to butadiene insertion into the Mt−allyl bond in systems comprising an ancillary Cp ligand. The transition states **4a** and **4b** have been obtained using the *endo*−*endo* monomer coordinated intermediate **2a** as starting point, while the transition states **4c** and **4d** have been obtained using the *endo*−*exo* monomer coordinated intermediate **2c** as starting point. Distances are in Å and energies are in kcal/mol.

obtained by approaching C1 of butadiene to the terminal and the internal allyl carbons, respectively. All four transition states present a distance between the two reactant carbons close to 2.1 Å.

The four transition states of Figure 4 (**4a**−**4d**) lead to monomer free species equal to those of Figure 1 (**1a**−**1d**), but with one additional monomer unit. In fact, it is already possible to define the chiralities of the incipient η^3 allyl group (C4−C3−C2) and of the η^2 backbiting double bond (C2′−C3′). The lowest energy transition state **4a** corresponds to 1,4-*like* insertion. The 1,2-*like* and 1,2-*unlike* transition states **4d** and **4b** present only slightly larger energies (≈1 kcal/mol), while the 1,4-*unlike* transition state **4c** is strongly unfavored and presents the worse coordination of the incipient backbiting of the double bond (C2′−Ti = 2.77 Å; C3′−Ti = 2.40 Å). The long Ti−C2′ distance is due to unfavorable steric interactions between C1′ (and its substituents) and Cp atoms (shortest distances are 3.2 and 3.35 Å). The energy increases with respect to the monomer coordinated intermediates **2a** and **2b** are small. For instance, the calculated energy barrier for the 1,4-*like* insertion is of only 3 kcal/mol.

Discussion

The approximate free energy profiles relative to *cis*-1,4- and 1,2-butadiene polymerizations, including the calculated diastereoisomeric monomer free intermediates of Figure 1, the monomer coordinated intermediates of Figure 2, and the insertion transition states of Figure 4, are shown in Figure 5. For the sake of simplicity, the two monomer coordinated species with *exo* monomer coordination and the corresponding four insertion transition states of high energy have not been shown in the scheme. The free energy profiles have been sketched in the rough assumption that the loss of entropy associated with monomer coordination is of 10 kcal/mol. It seems reasonable to assume that the $-T\Delta S$ contribution to the free energy of diene complexation to a group 4 metal atom in these catalysts is at least equal to 10 kcal/mol; that is the value observed[42] as well as calculated[43] at 300 K for olefin coordination to Ni and Pd compounds.

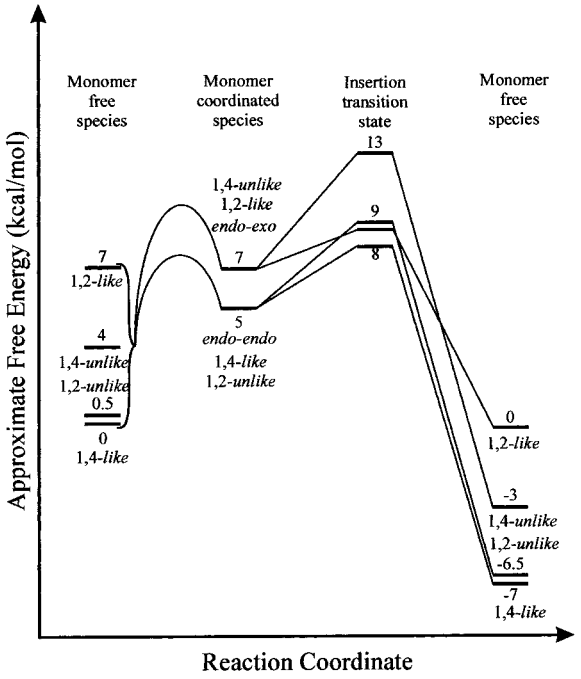

Figure 5. Energy profile relative to butadiene insertion into the Mt−allyl bond in models comprising an ancillary Cp ligand.

Since detailed calculations on the mechanism of monomer coordination were not performed, the energy barriers for monomer coordination have been only sketched in Figure 5, by showing that all the monomer free species would preferentially lead to the monomer coordinated species **2a**, which presents an *endo* allyl coordination. In fact, the barriers leading to the lower energy *endo*−*endo* intermediate **2a** are expected to be lower, also due to the maintenance of the *endo* allyl coordination already present in all the low-energy monomer free species of Figure 1.

The first thing worthy to note is that an easy reaction path connects the minimum-energy 1,4-*like* and 1,2-*unlike* intermediates on the left (reactants side) to the same intermediates on the right (products side). Both reaction paths evolve through the most stable *endo*−*endo* monomer coordinated intermediate and through low-energy transition states relative to the insertion reaction. It is also noteworthy that the most stable *endo*−*endo* monomer coordinated intermediate can be reached from and leads to the low-energy 1,4-*like* and 1,2-*unlike* reactants and products, respectively, without severe rearrangements of both the allylic chain end and of the monomer. With regard to the chemoselectivity, it has to be noted that starting from the *endo*−*endo* monomer coordinated intermediate, the lowest energy transition state for the insertion reaction corresponds to the 1,4-*like* enchainment.

The relative energies of the diastereoisomeric monomer free intermediates of Figure 1, and the low-energy reaction paths just described are in qualitative agreement with several experimental facts. In particular, systems based on $CpTiX_3$ (X = Cl,[44−45] F,[45] CH_3,[45] OR[46]) polymerize butadiene to products containing prevailingly 1,4 units (∼85%) and 1,2 units (∼10%), whose ratio is in qualitative agreement with the energy difference between the monomer free structures **1a** and **1b** and between the insertion transition states **4a** and **4b**. Moreover, the small energy difference between intermediates **1a** and **1b** as well as transition states **4a** and **4b**, which lead to 1,4 and 1,2 enchainments, respectively, could be responsible of the strong dependence of chemoselectivity on the kind of diene monomer.[44]

As for the stereoselectivity, the frequently observed syndiotacticity, for 1,2 polydienes, and the frequently observed isotacticity for *cis*-1,4 polymers (of 4-substitued dienes) by using catalytic systems based on $CpTiX_3$ (X = F, Cl, CH_3), Cp^*TiCl_3, Cp^*TiCl_2, Cp_2TiCl_2, and Cp_2TiCl,[44,47] well agrees with the lower energy of 1,2-*unlike* and 1,4-*like* monomer free intermediates with respect to 1,2-*like* and 1,4-*unlike* intermediates, with the low-energy of the *endo*−*endo* monomer coordinated intermediate, and with the low-energy barriers required to have both 1,4-*like* and 1,2-*unlike* insertions from the *endo*−*endo* coordinated intermediate.

The very high energies of the transition states corresponding to insertion of *exo* coordinated dienes indicate that direct insertion from the monomer coordinated intermediates **2a′** and **2b′** is unfeasible. Moreover, since the monomer free intermediates that are obtained starting from the *endo*−*endo* and *endo*−*exo* geometries **2a** and **2b** are identical to those obtained from the *exo*−*exo* and *exo*−*endo* geometries **2a′** and **2b′**, respectively, the latter intermediates can be considered not relevant for diene polymerization. This kind of result was already pointed out by simple molecular mechanics calculations[13] and is in good agreement with recent density functional studies calculations relative to dienes polymerization with Ni(II)-based catalytic systems.[12]

Experimental data on the activation energy of butadiene polymerization by these catalytic systems are not available. However, for the same catalytic systems the apparent activation energy for styrene polymerization (much faster than butadiene polymerization) has been evaluated as 7.6 kcal/mol.[48] Hence, the low-energy barriers for insertion of *endo* coordinated dienes we have calculated seem to confirm the previous suggestion that the transition state for diene polymerization would generally correspond to that relative to monomer coordination.[14]

In summary, the results of our calculations on model sites including a Cp ancillary ligand, schematically collected in Figure 5, suggest that the stereoselectivity (1,2-*like* vs 1,2-*unlike* as well as 1,4-*like* vs 1,4-*unlike*) could be essentially related to energy differences between monomer free intermediates, which in the framework of the mechanism depicted in Figure 5 should correspond to the resting state, while the chemoselectivity could be essentially related to energy differences between the insertion transition states.

Models Not Including an Ancillary Ligand (Mechanism Involving Two Backbiting Double Bonds). *Monomer Free Intermediates*. The conformational requirements, for the simultaneous coordination of the terminal allyl group and the two backbiting

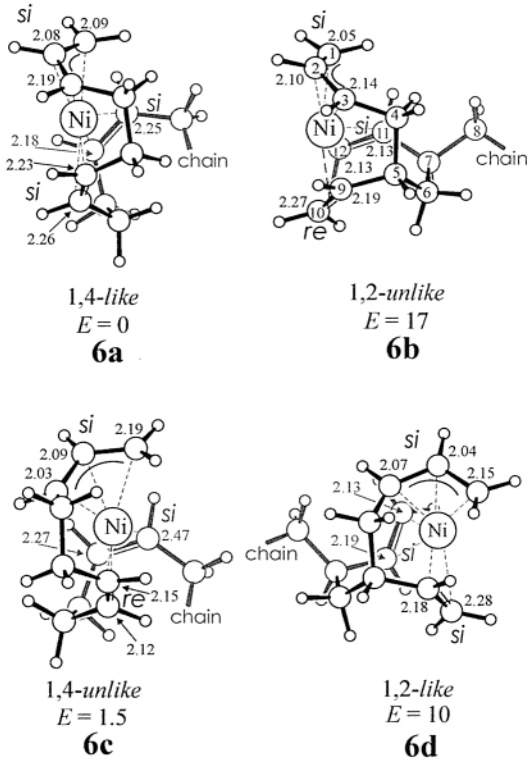

Figure 6. Minimum-energy geometries of the monomer free intermediates not including an ancillary ligand. The allylic-type chain end is η^3 coordinated to the metal, while two double bonds of the chain are η^2 coordinated (double backbiting) to the metal. Distances are in Å and energies are in kcal/mol. The gray atoms and bonds are under the metal.

double bonds, are strict and, of course, even more than those relative to models involving only one backbiting double bond.

The minimum-energy geometries of the diastereoisomeric monomer free intermediates not including an ancillary ligand, and presenting a double backbiting of the growing chain, are shown in Figure 6. To locate these conformations, s-*cis* coordinated butadiene has been inserted into polydiene backbiting chains analogous to those of Figure 1. Further attempts to locate different conformations, satifying the requirement of the double backbiting coordination for the considered configurations, were unsuccessful. Structures **6a** and **6c** correspond to the 1,4-*like* and *unlike* enchainments, while structures **6d** and **6b** correspond to the 1,2-*like* and *unlike* enchainments, respectively. The 1,2 monomer free intermediates **6b** and **6d** have energies which are significantly higher with respect to those relative to the 1,4 intermediates **6a** and **6c**. These higher energies are essentially related to the lower flexibility of the 1,2 intermediates, for which a lower number of carbon atoms (4 vs 6) separates the allyl group from the more distant backbiting double bond.

Monomer Coordinated Species. The minimum-energy intermediates presenting a s-*cis* η^4 coordinated butadiene and an *anti* η^3 and η^2 (backbiting) coordinated 1,4 growing chain are shown in Figure 7. Structures **7a** and **7b** present an *exo* and *endo* diene coordination to the metal and as a consequence of the reaction of C1 (of diene) with C4′ (of allyl) lead to 1,4-*like* and 1,4-*unlike* enchainments, respectively. Similar minimum-energy intermediates corresponding to the growing chain obtained by a 1,2 insertion have been also found. However,

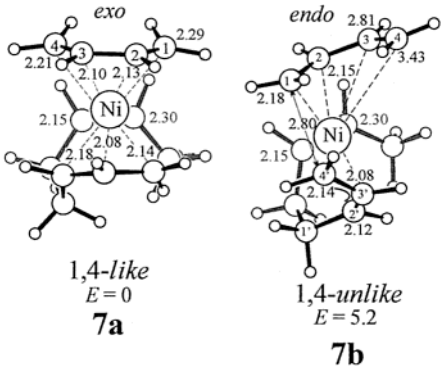

Figure 7. Minimum-energy geometries of the monomer coordinated intermediates not including an ancillary ligand. The allylic-type chain end is η^3 coordinated to the metal, while the closest double bond of the chain is still η^2 coordinated (backbiting) to the metal. The butadiene is s-*cis* η^4-coordinated (*endo* or *exo*) to the metal. Distances are in Å and energies are in kcal/mol.

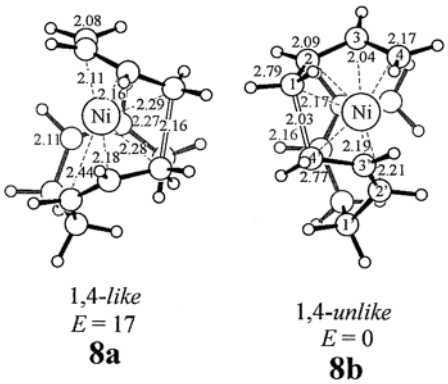

Figure 8. Geometries of the transition states that lead to 1,4-butadiene insertion into the Mt−allyl bond in systems not including an ancillary ligand. The transition states **8a** and **8b** corresponding to 1,4-*like* and 1,4-*unlike* intermediates have been obtained using the monomer coordinated intermediates **7a** and **7b** as starting points, respectively. Distances are in Å and energies are in kcal/mol.

due to the very high energy of the corresponding free monomer species **6b** and **6d**, they are not shown.

The 1,4-*like* intermediate **7a** is more stable of 5.2 kcal/mol with respect to the 1,4-*unlike* intermediate **7b**. The higher energy of the latter intermediate is related to the more hindered diene coordination which is essentially η^2 rather than the usual η^4 coordination. In fact, the calculated distances between diene carbons and the metal for 1,4-*unlike* monomer coordinated intermediate are C1−M = 2.18, C2−M = 2.15, C3−M = 2.81, and C4−M = 3.43 Å, while for the 1,4-*like* monomer coordinated intermediate these distances are C1−M = 2.26, C2−M = 2.13, C3−M = 2.10, and C4−M = 2.21 Å.

The achievement of the monomer coordinated intermediate **7b** from the minimum-energy monomer free intermediate **6c** implies a reduction of energy of nearly 10 kcal/mol, due to the s-*cis* coordination of the monomer which compensates the removal of the backbiting. Moreover, the monomer coordinated species **7b** (1,4-*unlike*) with *n*-inserted units is 8.6 kcal/mol higher in energy with respect to the monomer free species **6c** with $n + 1$ inserted units. It is worth noting that, for this Ni(II)-based catalyst, the calculated energy reduction corresponding to 1,4 insertion in a polydienylic chain, 18.6 kcal/mol, is in very good agreement with the experimental values of heats of polymerization ($\Delta H_{1,4\ cis}$ = 18.6 kcal/mol).[41]

Transition States for Monomer Insertion. The transition states corresponding to monomer insertions leading to 1,4-*like* and 1,4-*unlike* enchainments are compared in Figure 8. As already calculated for the models of the previous section, high-energy barriers are calculated for the insertion involving an *exo* coordinated diene (1,4-*like*). In fact, the calculated energy of the transition state relative to the 1,4-*like* insertion, **8a**, is 17 kcal/mol higher in energy than the transition state for 1,4-*unlike* insertion, **8b**. The transition state structure **8b** corresponding to the 1,4-*unlike* insertion is very similar to the corresponding monomer coordinated intermediate 7**b**. They mainly differ in distances between C1 and C4′, which are 2.8 and 2.03 Å in the monomer coordinated species **7b** and in the transition state structure **8b**, respectively.

Discussion

Density functional studies relative to butadiene polymerization with Ni(II)-based catalytic systems have been already reported by Taube and co-workers.[24] Although those studies were mainly focused on the *syn*−*anti* equilibrium of the coordinated allyl group of the growing chain, some of the calculated intermediates and transition states can be compared with those modeled in the previous sections. In particular, the geometry of the 1,4-*like* monomer free intermediate **6a** is very similar to the geometry presented by Taube in Figure 4 of ref 24 (**2a**-SSb(c)). Moreover, the geometry and the energy relative to the monomer coordinated species **7a** and **7b** are very similar to those of the intermediates shown in Taube's Figure 5 (**4a**-SSf and **4a**SPb, respectively). Finally, also the geometry and the energies relative to the transition states 1,4-*like* **8a**, and 1,4-*unlike* **8b**, are comparable with those presented in Taube's Figure 6 (**5a**-SSf and **5a**-SPb, respectively).

The geometry of the diastereoisomeric monomer free intermediates shown in Figure 6 are not comparable with the experimental data relative to complexes characterized by X-ray diffraction. In fact, the reported complexes involving two backbiting double bonds always present a *syn* (instead of an *anti*) coordinated allyl group.[28b,30]

Approximate free energy profiles relative to 1,4-butadiene polymerizations, including the calculated diastereoisomeric monomer free intermediates of Figure 6, the monomer coordinated intermediates of Figure 7, and the insertion transition states of Figure 8, are shown in Figure 9. For the sake of simplicity, as for the free energy profiles relative to 1,2 polymerizations of butadiene, only the high-energy monomer free intermediates have been shown in Figure 9.

The relative energies of the monomer free intermediates well account for the high chemoselectivity of Ni(II)-based catalytic systems. In particular, Ni(II)-based catalytic systems such as Ni(acac)$_3$−MAO,[49] AlEt$_3$−Ni octanoate−BF$_3$ phenolate,[50] and AlEt$_3$−Ni octanoate−BF$_3$ OEt$_2$,[51] as well as those including doubly backbiting $C_{12}H_{19}$ groups coordinated to the metal,[28b,30] polymerize diene monomer to products containing essentially only *cis*-1,4 units.

With regard to the stereoselectivity, the much lower energy of the transition states for the achievement of the 1,4-*unlike* enchainment with respect to the 1,4-*like* one well accounts for the syndiotacticity experimentally observed for the *cis* 1,4 polymers of 4-substituted dienes

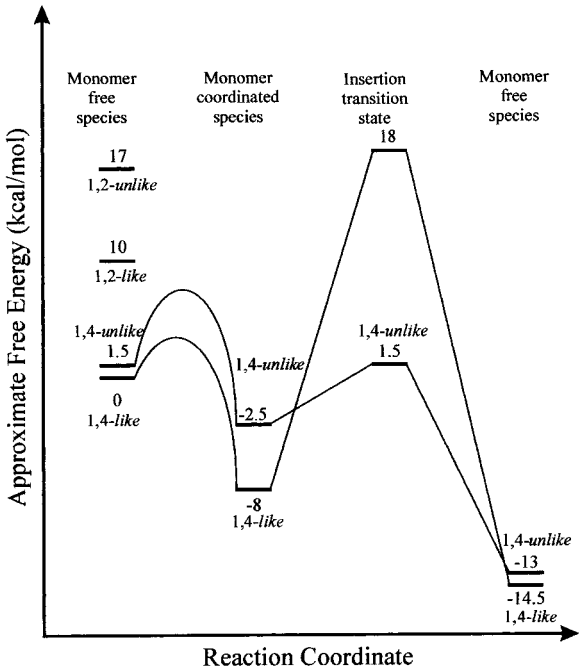

Figure 9. Energy profile relative to butadiene insertion into the Mt−allyl bond in systems not including an ancillary ligand. Because of the very high energy of the free monomer species, the energy relative of the 1,2 monomer coordinated intermediates and the corresponding transition states are not shown.

by using catalytic systems as $Ni(acac)_3$−MAO[49] and $AlEt_3$−Ni octanoate−BF_3 phenolate.[51]

Conclusions

The mechanisms of stereoselectivity and chemoselectivity in Ziegler−Natta polymerizations of conjugated dienes have been investigated by density functional methods, in the framework of the widely accepted polymerization scheme involving *anti*-allyl coordination of the growing chain.

The monomer coordinated and monomer free intermediates that, according to the present calculations, are suitable for *cis* 1,4 and 1,2 polymerizations of butadiene in the presence of a Cp ancillary ligand, are collected in Figure 10A. Most insertions would occur starting from the *endo*−*endo* monomer coordinated intermediate, that is, from s-*cis* η^4 coordinated monomers with their concavity oriented toward the terminal allyl group of the growing chain. These insertions would lead, through least nuclear motions, to both 1,4-*like* and 1,2-*unlike* monomer free intermediates.

Intermediates that, according to the present calculations, are energetically feasible for diene polymerization in the framework of a mechanism involving two backbiting double bonds of the growing chain, as assumed for Ni(II)-based catalytic systems, are shown in Figure 10B. Most insertions would occur from the *endo* monomer coordinated intermediate, that is, again from a s-*cis* η^4 coordinated monomer with its concavity oriented toward the terminal allyl group of the growing chain. These insertions would lead, through least nuclear motions, essentially only to 1,4-*unlike* monomer free intermediate.

As discussed in detail in the Discussion sections, these kinds of models are able to rationalize several experimental data relative to the mechanisms of stereoselectivity and chemoselectivity in Ziegler−Natta polymerizations of conjugated dienes.

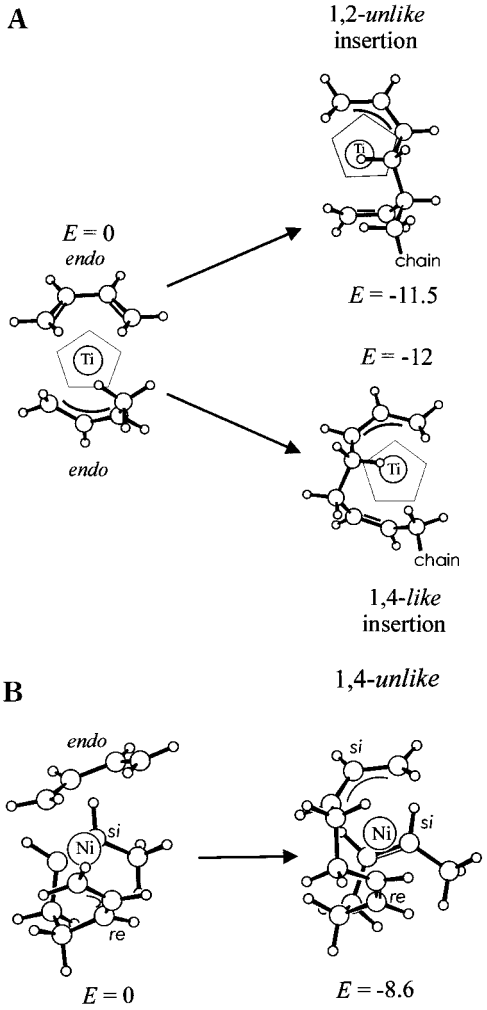

Figure 10. (A, top) Geometries of the coordination intermediate, **2a**, and of monomer free intermediates **1a** and **1b**, corresponding to 1,2-*unlike* and 1,4-*like* diene insertions into the Mt−allyl bond in models comprising an ancillary ligand. (B, bottom) Geometries of the coordination intermediate, **7b**, and of the monomer free intermediates, **6c**, corresponding to 1,4-*unlike* insertions into the Mt−allyl bond in models not including an ancillary ligand and including two backbiting double bonds.

Since the calculated geometry of the intermediates and of the transition states as well as the general pattern of the energy profiles (like those of Figures 5 and 9) are poorly dependent on the nature of the metal and on the nature of the ancillary ligand, we suggest a more general working hypothesis. Models including an ancillary ligand (for which the backbiting of only one double bond is feasible in the monomer free intermediates) would lead to both 1,4-*like* and 1,2-*unlike* enchainments, while models not including an ancillary ligand (for which the backbiting of two double bonds is feasible in the monomer free intermediates) would essentially lead to 1,4-*unlike* enchainments only.

Of course, this kind of general mechanism would not be valid in the presence of *syn*-allyl coordination of the growing chain. To achieve a more general mechanism of stereoselectivity and chemoselectivity in diene polymerizations, models presenting the *syn*-allyl coordination of the growing chain will be considered in future studies.

Acknowledgment. We thank Prof. Porri of the Polytechnic of Milano, Profs. Zambelli and Longo of the

University of Salerno, Dr. Fusco of the Institute Guido Donegani of Enichem, and Prof. Corradini of the University of Naples for useful discussions. This work was supported by the of MURST of Italy, Grant PRIN-2000, and by Consiglio Nazionale delle Richerche.

Supporting Information Available: Experimental and calculated Cartesian coordinates of the neutral complexes $Cp_2Ti(C_5H_9)$ and $CpZr(C_3H_5)(C_4H_6)$ considered in test calculations and tables containing their main distances and angles. This material is available free of charge via the Internet at http://pubs.acs.org.

References and Notes

(1) Porri, L.; Natta, G.; Gallazzi, M. C. *Chim. Ind. (Milan)* **1964**, *46*, 428.
(2) Natta, G.; Porri, L.; Carbonaro, A.; Greco, A. *Makromol. Chem.* **1964**, *71*, 207.
(3) Wilke, G.; Bogdanovich, B.; Hardt, P.; Heimbach, P.; Keim, W.; Kromer, M.; Oberkirch, W.; Tanaka, K.; Steinrucke, E.; Walter, D.; Zimmermann, H. *Angew. Chem., Int. Ed. Engl.* **1966**, *5*, 151.
(4) Marconi, W. In *Stereochemistry of Macromolecules*; Ketley, A. D., Ed.; Dekker: New York, 1967; Vol. 1, p 239.
(5) Natta, G.; Porri, L. In *Polymer Chemistry of Synthetic Elastomers*; Kennedy, J. P., Tornquist, E., Eds.; Wiley-Interscience: New York, 1969; Part II, p 597.
(6) Teyssie, P.; Dawans, F. *The Stereo Rubbers*; Saltman, W. M., Ed.; Wiley: New York, 1977; p 79.
(7) Porri, L. In *Structural Order in Polymers*; Ciardarelli, F., Giusti, P., Eds.; Pergamon Press: Oxford, U.K., 1981; p 51.
(8) Porri, L.; Giarrusso, A. In *Comprehensive Polymer Science*; Eastmond, G. C., Ledwith, A., Russo, S., Sigwalt, P., Eds.; Pergamon Press: Oxford, U.K., 1989; Vol. 4, Part II, p 53.
(9) Porri, L.; Giarrusso, A.; Ricci, G. *Prog. Polym. Sci.* **1991**, *16*, 405.
(10) Taube, R.; Windisch, H.; Maiwald, S. *Macromol. Symp.* **1995**, *89*, 393.
(11) Woo, T.; Fan, L.; Ziegler, T. *Organometallics* **1994**, *13*, 2252.
(12) Tobish, S.; Bögel, H.; Taube, R. *Organometallics* **1996**, *15*, 3563.
(13) Guerra, G.; Cavallo, L.; Corradini, P.; Fusco, R. *Macromolecules* **1997**, *30*, 677.
(14) Peluso, A.; Improta, R.; Zambelli, A. *Organometallics* **1998**, *19*, 411.
(15) Natta, G.; Giannini, U.; Pino, P.; Cassata, A. *Chim. Ind. (Milan)* **1965**, *47*, 525.
(16) Taube, R.; Wache, S.; Sieler, J. *Organomet. Chem.* **1993**, *459*, 335.
(17) Ciajolo, R.; Jama, M. A.; Tuzi, A.; Vitagliano, A. *J. Organomet. Chem.* **1985**, *295*, 233.
(18) Corradini, P.; Guerra, G.; Jama, M. A.; Zhi, G.; Tuzi, A. *Polym. Commun.* **1985**, *26*, 175.
(19) Allegra, G.; Lo Giudice, F.; Natta, G.; Giannini; U.; Fagherazzi; G.; Pino, P. *Chem. Commun.* **1967**, 1263.
(20) (a) Corradini, P.; Guerra, G. *Prog. Polym. Sci.* **1991**, *16*, 239. (b) Corradini, L.; Cavallo, L.; Guerra, G. In *Metallocene Based Polyolefins, Preparation, Properties and Technology*; Scheirs, J., Kaminsky, W., Eds.; John Wiley & Sons: New York, 2000; Vol. 2, p 3. (c) Resconi, L.; Cavallo, L.; Fait, A.; Piemontesi, F. *Chem. Rev.* **2000**, *100*, 1253.
(21) Angermund, K.; Fink, G.; Jensen, V. R.; Kleinschmidt, R. *Chem. Rev.* **2000**, *100*, 1457.
(22) Peluso, A.; Improta, R.; Zambelli, A. *Macromolecules* **1997**, *30*, 2219.
(23) Taube, R. *Organometallics* **1998**, *17*, 1177.
(24) Tobisch, S.; Taube, R. *Organometallics* **1999**, *18*, 8, 5204.
(25) Tobisch, S.; Taube, R. *Organometallics* **1999**, *18*, 3045.
(26) Erker, G.; Berg, K.; Krüger, C.; Müller, G.; Angermund, K.; Benn, R.; Schroth, G. *Angew. Chem., Int. Ed. Engl.* **1984**, *23*, 455.
(27) Hanson, K. R. *J. Am. Chem. Soc.* **1966**, *88*, 2731.
(28) (a) Taube, R.; Gehrke, J.-P.; Böhme, P.; Köttinz, J. *J. Organomet. Chem.* **1990**, *395*, 341. (b) Taube, R.; Böhme, P.; Gehrke, J.-P. *J. Organomet. Chem.* **1990**, *399*, 327.
(29) Sieler, J.; Kempe, R.; Wache, S.; Taube, R. *J. Organomet. Chem.* **1993**, *455*, 24.
(30) Sieler, J.; Kempe, R.; Wache, S.; Taube, R. *J. Organomet. Chem.* **1993**, *456*, 131.
(31) Brookhart, M.; Cox Cloke, F. G. N.; Green, J. C.; Green, L. M. H.; Hare, P. M. *J. Chem. Soc., Dalton Trans.* **1985**, 432.
(32) Baerends, E. J.; Ellis, D. E.; Ros, P. *Chem. Phys.* **1973**, *2*, 41.
(33) Baerends, E. J.; Ros, P. *Chem. Phys.* **1973**, *2*, 52.
(34) Vosko, S. H.; Wilk, L.; Nusair, M. *Can. J. Phys.* **1980**, *58*, 1200.
(35) Becke, A. D. *Phys. Rev. B* **1986**, *34*, 7406.
(36) Perdew, J. P. *Phys. Rev* **1988**, *38*, 3098.
(37) (a) Lhorenz, J. C. W.; Woo, T. K.; Ziegler, T. *J. Am. Chem. Soc.* **1995**, *117*, 12793. (b) Deng, L.; Woo, T. K.; Cavallo, L.; Margl, P. M.; Ziegler, T. *J. Am. Chem. Soc.* **1997**, *119*, 6177. (c) Cavallo, L.; Guerra, G.; Corradini, P. *J. Am. Chem. Soc.* **1998**, *120*, 2428. (d) Margl, P. M.; Deng, L.; Ziegler, T. *J. Am. Chem. Soc.* **1998**, *120*, 5517. (e) Guerra, G.; Longo, P.; Corradini, P.; Cavallo, L. *J. Am. Chem. Soc.* **1999**, *121*, 8651. (f) Milano, G.; Guerra, G.; Pellecchia, C.; Cavallo, L. *Organometallics* **2000**, *19*, 1343. (g) Longo, P.; Grisi, F.; Guerra, G. Cavallo, L. *Macromolecules* **2000**, *33*, 4647.
(38) (a) Minieri, G.; Corradini, P.; Zambelli, A.; Guerra, G.; Cavallo, L. *Macromolecules* **2001**, *34*, 2459. (b) Minieri, G.; Corradini, P.; Zambelli, A.; Guerra, G.; Cavallo, L. *Macromolecules* **2001**, *34*, 5379.
(39) Jensen, V. R.; Borve, K. J. *J. Comput. Chem*, **1991**, *19*, 94.
(40) Helmholdt, R. B.; Jellimek, F.; Martin, H. A.; Vos, A. *Rec. J. R. Neth. Chem. Soc.* **1967**, *86*, 1263.
(41) Roberts, D. E. *J. Res. Natl. Bur. Stand.* **1950**, *44*, 221.
(42) Rix, F. C.; Brookhart, M.; White, P. S. *J. Am. Chem. Soc.* **1996**, *118*, 4746.
(43) (a) Margl, P.; Deng, L.; Ziegler, T. *Organometallics* **1998**, *17*, 933. (b) Musaev, D. G.; Froese, R. D. J.; Svensson, M.; Morokuma, K. *J. Am. Chem. Soc.* **1997**, *119*, 367.
(44) Longo, P.; Oliva, P.; Proto, A.; Zambelli, A. *Gazz. Chim. Ital.* **1996**, *126*, 377.
(45) Zambelli, A.; Caprio, M.; Grassi, A.; Bowen, Daniel, E. *Macromol. Chem. Phys.* **2000**, *201* (4), 393.
(46) Ricci, G.; Porri, L.; Giarrusso, A. *Macromol. Symp.* **1995**, *89*, 383.
(47) Ricci, G.; Italia, S.; Porri, L. *Macromolecules* **1994**, *27*, 868.
(48) Ishihara, N.; Kuramoto, M.; Uoi, M. *Macromolecules* **1988**, *21*, 3356.
(49) Oliva, L.; Longo, P.; Grassi, A.; Ammendola, P.; Pellecchia, C. *Mackromol. Chem., Rapid Commun.* **1990**, *11*, 519.
(50) (a) Beebe, D. H.; Gordo, C. E.; Thudium, R. N.; Throckmorton, M. C.; Hanlon, T. L. *J. Polym. Sci., Polym. Chem. Ed.* **1978**, *16*, 2285. (b) Beebe, D. H.; Gordo, C. E.; Thudium, R. N.; Throckmorton, M. C.; Hanlon, T. L. *J. Polym. Sci., Polym. Chem. Ed.* **1978**, *16*, 2285.
(51) Saltman, W.; Kuzuma, L. J. *Rubber Chem. Technol.* **1972**, *45*, 1055.

MA010673H